Correspondence

Compact Planar Antennas for Short-Range Wireless Automotive Communication

Basim Al-Khateeb, Victor Rabinovich, Barbara Oakley, and Nikolai Alexandrov

***Abstract*—This paper describes several small printed circuit board planar antennas that can be integrated with amplifiers for short-range vehicle wireless communication. The antennas are designed for the 315-MHz frequency band, which is commonly used for control and security devices in the USA and Canada. Each antenna has dimensions of 50 × 70 mm (much less than the free-space wavelength $\lambda = 0.95$ m) and is implemented on FR-4 dielectric substrate. These investigated antennas were compared with respect to input impedance, radiation resistance, radiation efficiency, directivity, directionality, bandwidth, matching system complexity, and gain. This paper also includes experimental verification of the final antenna design in the vehicle. It is shown that the antenna diversity method can increase communication range for remote keyless entry systems.**

***Index Terms*—Miniature antenna, printed circuit board antenna, short-range wireless communication.**

I. Introduction

In recent years, the wireless communication market has expanded greatly. Wireless devices such as remote control engine start systems, remote keyless entry (RKE) systems, and automatic tolling systems are now considered "classical" devices for short-range vehicle wireless communication [1], [2]. Such control and security devices commonly use the 315-MHz frequency band in USA and Canada. In these systems, the antenna is a key component for system performance and size. Compact antennas have gained special attention over the past few years because of the possibilities they present for reduced-size, in comparison with conventional dipoles.

The communication range that can be achieved in a radio system depends strongly on antenna performance properties. The physical size is limited in many short-range devices (SRDs) for automotive applications; thus, the antenna must also be small. Yet, of course, size is vital to the antenna's performance. It is worthwhile to estimate the parameters of a variety of small antennas to guide the design of the best antenna for a particular application.

In this paper, we investigate and compare several planar printed circuit board miniaturized antennas for wireless automotive keyless entry applications. Such compact antennas can be integrated with low-noise amplifiers to extend short-range wireless communication. The different antenna geometries discussed here have dimensions limited to less than 50 × 70 mm, as dictated by customer requirements. These dimensions are much less than the wavelength. It should be noted that such antennas are limited in their application by narrow bandwidth (high quality factor), small radiation resistance, small gain, and small allowable tolerances for the matching system.

Manuscript received October 7, 2004; revised July 22, 2005 and November 9, 2005. The review of this paper was coordinated by Prof. R. Janaswamy.

B. Al-Khateeb is with DaimlerChrysler Corporation, Auburn Hills, MI 48326 USA.

V. Rabinovich and N. Alexandrov are with Tenatronics Ltd., Newmarket, ON L3Y 2R4, Canada (e-mail: research@tenatronics.ca).

B. Oakley is with the Department of Electrical and Systems Engineering, Oakland University, Rochester, MI 48309 USA.

Digital Object Identifier 10.1109/TVT.2006.877474

There are five main requirements for the antenna design.

1) The antenna should operate in the 315-MHz frequency range with a 300-kHz bandwidth and be printed on low-cost substrate FR-4.
2) Output antenna impedance must be 50 Ω.
3) An effective and low-cost matching circuit must be designed to provide minimum noise figure for the low-noise amplifier integrated with the antenna.
4) Each antenna must have a ground pad to be used as the second arm of the antenna and that can also serve as the amplifier ground following the antenna.
5) The antenna must provide reception over 360° in the horizontal plane.

Many papers have been devoted to compact printed antennas with different trace geometries; these papers have investigated radiation resistance, radiation efficiency, and input impedance [3]–[26]. Some of the antennas under investigation have been printed monopoles [3]–[6], some have had L-shaped configurations [7]–[10], and some have been meander line antennas [11]–[26]. The vast majority of these papers have been devoted to meander line antennas at frequency ranges above 500 MHz. Several small meander line antennas at frequencies below 500 MHz are discussed in [23]–[26]. The meander line antennas described in [23] and [24] are symmetrical meander line dipoles or monopoles placed on the infinite ground plane.

The fundamental principles of small antenna radiation are studied and described in [27]–[30]. These papers show the relationship between quality factor and bandwidth, quality factor and radiation efficiency, and gain and antenna size. The analytical expression for the impedance, radiation resistance, and antenna directionality for the wire loop antenna has been described in the fundamental monograph [31]. Tsukiji and Tou [32] investigate simple formulas for the impedance of the different wire loop antenna geometries: circular, square, rectangle, delta, and hexagonal. Such studies are very useful for antenna designers. The analytical formulas for the gain, radiation efficiency, and bandwidth shown in these papers provide excellent guides for rough estimations. On the other hand, only mathematical simulation and prototype design can give us the real parameters of a designed antenna for certain applications.

The optimal simulated antenna design presented in this paper was fabricated and measured together with an integrated amplifier in the DaimlerChrysler vehicle "Durango 2004." The measured radiation patterns are analyzed for several different antenna and radio frequency (RF) cable locations in the vehicle. Finally, the effect of the antenna diversity technique on communication range is presented.

II. Antenna Geometry

The geometries of the antennas investigated in this paper are shown in Fig. 1. All antennas use a ground pad for the antenna amplifier ground. The maximum antenna dimensions are 50 × 70 mm. A planar printed loop antenna [Fig. 1(a)] was examined as the first configuration for keyless entry applications described in this paper. The second type of antenna, as shown in Fig. 1(b), was a printed monopole antenna. The third antenna type [Fig. 1(c)] was an L-inverted antenna. The fourth and fifth antenna types [Fig. 1(d) and (e)] were planar printed meander line antennas. Meander line antennas are of particular interest because the folded wire length in a monopole antenna increases the

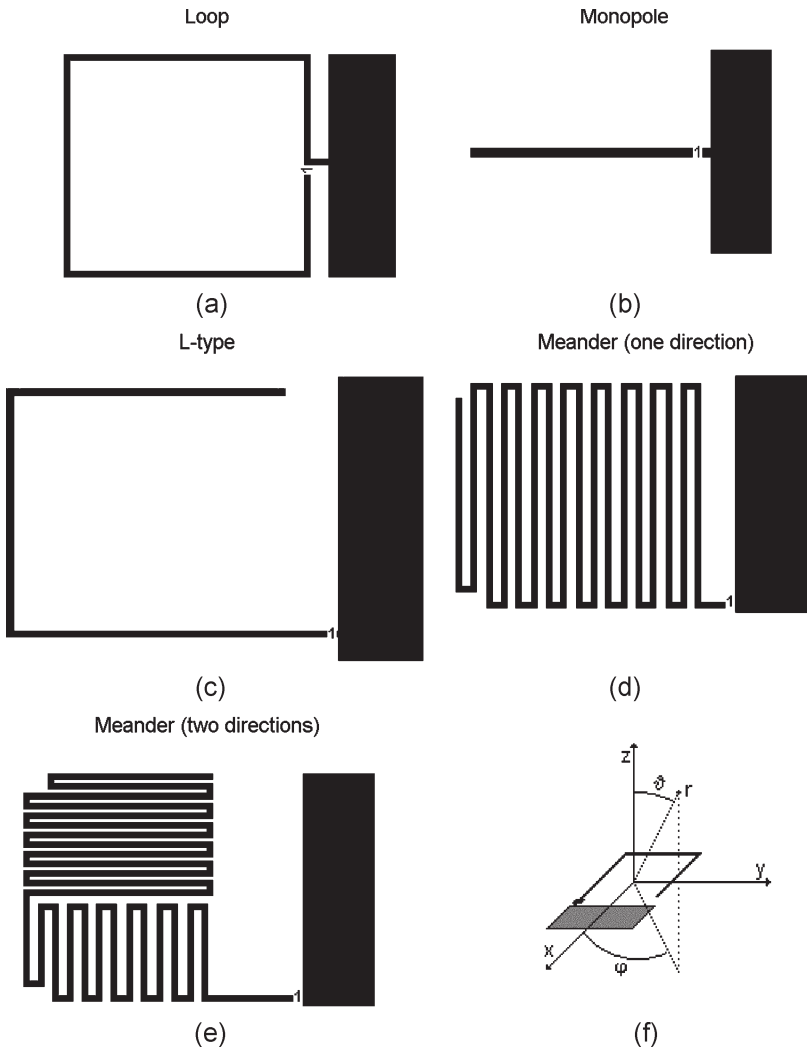

Fig. 1. Investigated antenna geometries.

radiation resistance and, consequently, the input impedance. It is a straightforward task to design a meander line that provides an antenna output impedance close to 50 Ω.

The antennas are printed on the front of a 1.6-mm-thick FR-4 substrate (with a relative permittivity of 4.4). The width of the printed antenna trace lines is 1 mm. Ground pads are used as the second "arm" on each of these antennas; the pads serve concomitantly as low-noise amplifier grounds. The low-noise amplifier located at the antenna trace line side increases the sensitivity of the receiver.

III. Main Antenna Performance

For this investigation, antenna parameters were studied using both simulation software and experimental measurements. Printed antenna parameters are often very difficult to compute using analytical expressions, but they can be estimated with the help of electromagnetic software or they can be determined experimentally. We used IE3D software for our antenna parameter simulation analysis [33]. IE3D is a full-wave method-of-moments-based electromagnetic simulator that solves the current distribution on three-dimensional (3-D) and multilayer structures of general shape. It has been widely used in the design of planar antennas, wire antennas, and other RF/wireless antennas [5]. The following three groups of parameters were computed for every antenna type: 1) input impedance, radiation resistance and loss resistance, radiation efficiency, and bandwidth; 2) matching to 50-Ω circuits for all antenna types and matching stability of voltage standing wave ratio (VSWR) when lumped elements are within tolerance values; and 3) directionality and gain. The antenna feed point is indicated by point 1 in Fig. 1.

The experimental antenna investigation consisted of two steps: The first step consisted of measuring the radiation pattern in the anechoic chamber without the vehicle. The second step involved the analysis of the antenna radiation pattern with the antenna mounted on a vehicle, which was in turn located on an outdoor automobile turntable (Tenatronics Ltd.). The antenna range instrumentation was controlled by a computer that drove the turntable rotation, controlled a spectrum analyzer, and transferred the measured data to the hard drive and printer. A data point was taken on the 0° elevation amplitude pattern every 2° as the turntable was rotated through a full 360° azimuth. Using the turntable in this fashion, we investigated antenna directionality, antenna gain, and residual noise of the active antenna. The effect on the antenna parameters of an external RF cable connection between the antenna and receiver was also examined.

IV. Simulation Results

A. Efficiency and Impedance

The radiation efficiency of an electrically small antenna is determined by the losses in the conductors, dielectrics, and other materials

TABLE I
INPUT IMPEDANCE, RADIATION AND LOSS RESISTANCE, EFFICIENCY, DIRECTIVITY, AND GAIN OF PRINTED PLANAR ANTENNAS

Antenna	Re(Z) Ohms	Im(Z) Ohms	R_r Ohms	R_l Ohms	η_a %	D_{xy} dBi	G_{xyo} dBi
Loop	23.96	911.4	3.57	20.39	14.9	1.8	-6.5
Monopole	5.61	-548.7	0.95	4.66	16.9	1.9	-5.8
L-type	4.64	-324.4	1.25	3.39	27.0	1.8	-3.9
Meander (one direction)	17.03	19.5	5.11	11.92	30.0	1.8	-3.4
Meander (two directions)	14.60	17.59	2.63	11.97	18.0	1.8	-5.6

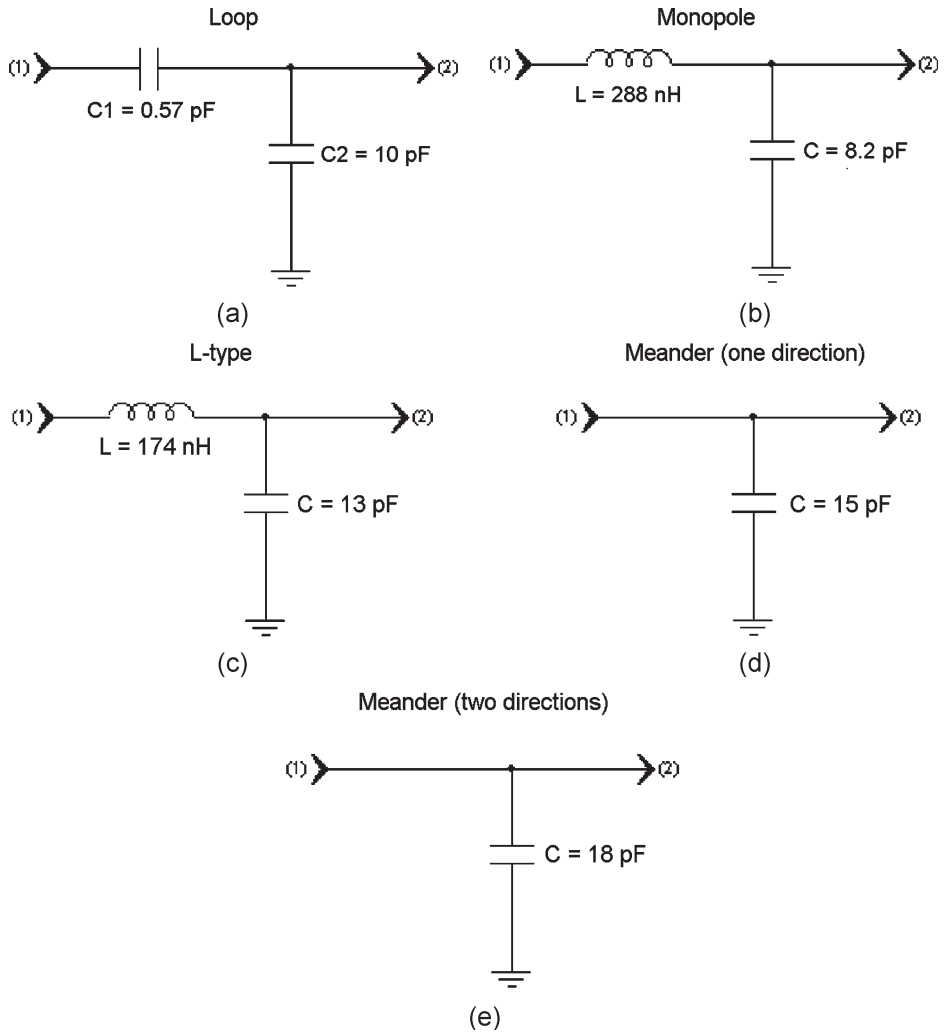

Fig. 2. Matching to 50-Ω impedance electrical circuits for different antenna geometries.

from which the antenna is constructed, as compared with radiation loss. This can be expressed as

$$\eta_a = \frac{R_r}{R_r + R_l} \tag{1}$$

where

η_a radiation efficiency of an antenna;
R_r radiation resistance;
R_l material loss resistance.

To provide the maximum transfer power into an antenna's driving point, a matching network is often required. The efficiency of the antenna and its matching network can be expressed as

$$\eta_s = \eta_a \cdot \eta_m \tag{2}$$

where η_s is the efficiency of the system (antenna and matching network) and η_m is the efficiency of the matching network including heat-ohmic loss within the network components and mismatching losses.

The efficiency system parameter affects the antenna gain. The ratio between antenna gain and directivity can be expressed as

$$G_a = \eta_s \cdot D \tag{3}$$

where D is the antenna directivity. Antenna bandwidth can be expressed as

$$BW = \Delta F / F \tag{4}$$

where F is the operating frequency and the calculated value ΔF is based on VSWR < 5.85 ($|S_{11}| \leq -3$ dB).

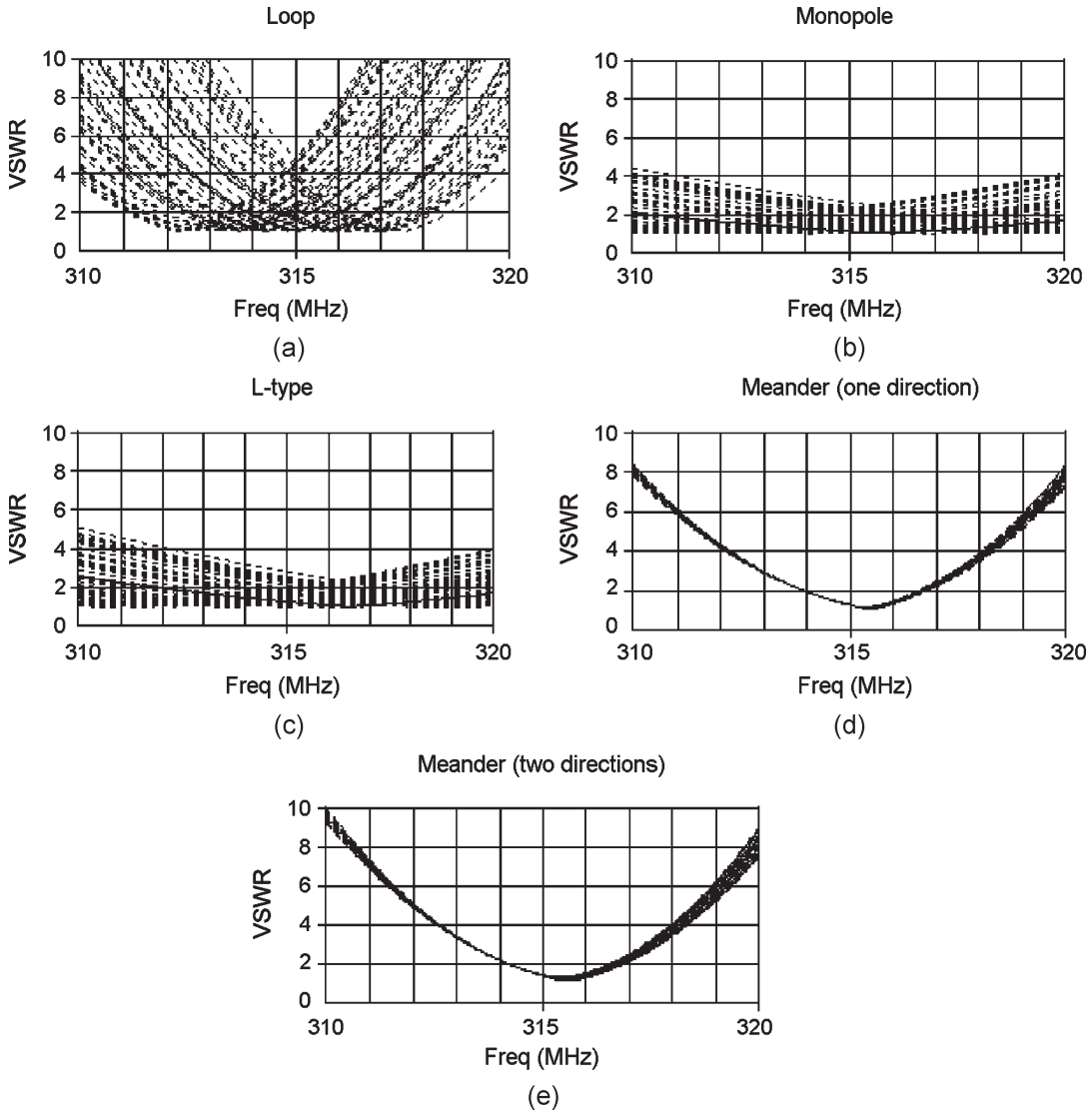

Fig. 3. Monte Carlo analysis results for the VSWR of the matching circuits with component tolerances within ±5%.

The simulated real $\mathrm{Re}(Z)$ and imaginary $\mathrm{Im}(Z)$ parts of the antenna input impedance, radiation resistance, loss resistance, and radiation efficiency before antenna matching to 50-Ω impedance are shown in Table I. Table I also shows the directivity D_{xy} and gain G_{xy0} in the xy plane for the electromagnetic field component $E_{\varphi}(\theta = 90^{\circ})$. Gain G_{xy0} is calculated for the condition $\eta_m = 1$. As shown in Table I, all antennas have approximately the same directivity in the xy plane. The meander line antenna shown in Fig. 1(d) has the highest gain value.

B. Matching Circuits

The matching circuit for each antenna type is shown in Fig. 2; these circuits were designed with the help of Genesys Software from Eagleware Corporation [34]. Inductor components have a quality factor value of 25, whereas capacitor components have a quality factor of 100. These values are chosen from the specifications of the TOKO Company, a leading manufacturer of surface-mounted components. To understand the variation of the VSWR values due to the within tolerance variation of the lumped matching elements from their nominal values, we used the Monte Carlo analysis option included in the Genesys Software. The Monte Carlo analysis evaluates circuit behavior with a random distribution of component values within specific limits. It is a statistical process that reveals whether production results will fall within acceptable limits or not. The Monte Carlo analysis supplies multiple responses, each generated with a pseudorandom set of component values based on the specified distribution and tolerances.

Results for uniform distribution values with component tolerances of ±5% are shown in Fig. 3. We can see from these results that both one- and two-directional meander antennas have the most stable VSWRs when matching components are within a tolerance of ±5%. This result can be explained very simply. The meander line antenna, when matched to 50 Ω, has a reduced number of components. Each component, of course, adds a new level of variability, as can be observed with the loop or monopole antenna. In reality, the meander line antenna is physically small but electrically large. Therefore, the matching circuit for meander line antenna is not as critical as that for the other antenna types shown in Fig. 1. The antennas of Fig. 1(a)–(c) have large reactance values before matching. Therefore, the ±5% tolerance for matching component values drops the VSWR to unacceptable values. Table II shows the main antenna parameters after matching the antenna output to the 50-Ω impedance.

TABLE II
PARAMETERS OF PLANAR ANTENNAS WITH OUTPUT MATCHING TO 50-Ω IMPEDANCE

Antenna	Re(Z) Ohms	Im(Z) Ohms	R_r Ohms	R_l Ohms	η_s %	VSWR	BW %	G_{xy} dBi
Loop	49.8	2.0	7.3	42.5	14.7	1.1	2	-6.5
Monopole	44.4	1.3	1.5	42.9	3.3	1.1	10	-12.9
L-type	39.8	2.1	2.7	37.1	6.8	1.3	8	-9.9
Meander (one direction)	39.2	-0.9	11.7	27.5	29.9	1.3	2.5	-3.4
Meander (two directions)	35.5	-2.5	6.4	29.1	17.9	1.4	2.5	-5.7

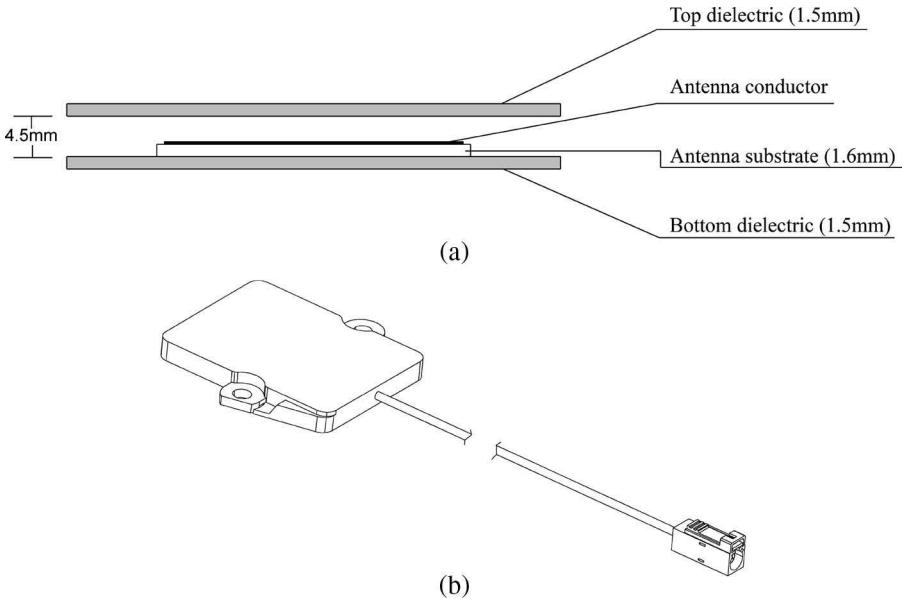

Fig. 4. (a) Meander line antenna between two infinite plastic plates (ABS material, $e = 3.4$). (b) Antenna in plastic case for vehicle applications.

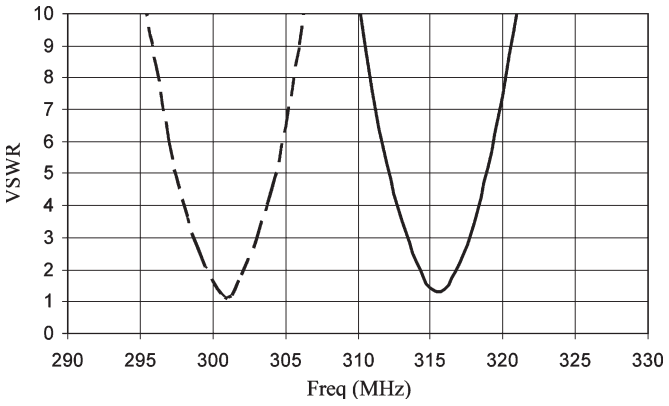

Fig. 5. Calculated VSWR of an antenna placed between two dielectric plates without tuning to 315 MHz (dashed curve) and when tuned to 50 Ω at 315 MHz (solid curve).

The small-loop antenna has a high quality factor, with concomitant narrow bandwidth. Therefore, small-loop antenna matching within the tolerance of the lumped elements is a difficult task. Matching circuits for monopole and L-type antennas incorporate an inductor; due to the low quality factor of an inductor ($Q = 25$), these antennas, when matched to the 50-Ω, have reduced gain. The gain of both meander line antennas exceeds the gain of the loop, monopole, and L-type antennas. The bandwidth of the antennas under investigation is not a very critical factor for this application.

C. Meander Line Antenna in a Plastic Case

The flat printed antenna intended for remote control vehicle applications has a plastic case built of radio-transparent material. The case is fixed to the car body interior and protects the antenna from damage in the car. Naturally, the radio-transparent dielectric material changes the antenna resonance frequency. Using IE3D software, we computed the influence of the infinite plastic plates (ABS material, dielectric constant $\varepsilon = 3.4$) on the VSWR, with the meander line antenna [Fig. 1(e)] sandwiched between the plates [Fig. 4(a)]. Mathematical simulation results (Fig. 5) show that the resonance frequency of such an antenna is shifted into a lower frequency range than that of an antenna without such radio-transparent material added. Simply changing the matching capacitor value from 18 to 20 pF provides the best matching results when the antenna is placed between infinite plastic plates. A sample antenna in a plastic case, as for vehicle applications, is shown in Fig. 4(b).

V. PASSIVE ANTENNA RADIATION PATTERNS

Computed radiation patterns for the electromagnetic field components $E_\varphi(\varphi, \theta = 90°)$ and $E_\theta(\theta, \varphi = 90°)$ are shown in Fig. 6(a)–(e). Antenna geometry location with respect to rectangular (x, y, and z) and polar (r, θ, and φ) coordinates are shown in Fig. 1(f). The dashed line curve in Fig. 6(f) is measured in the anechoic chamber, with the radiation pattern indicated in the xy plane [field component $E_\varphi(\varphi, \theta = 90°)$]. The antenna ground plane is printed on the bottom as well as on top of the substrate. As can be observed, the agreement

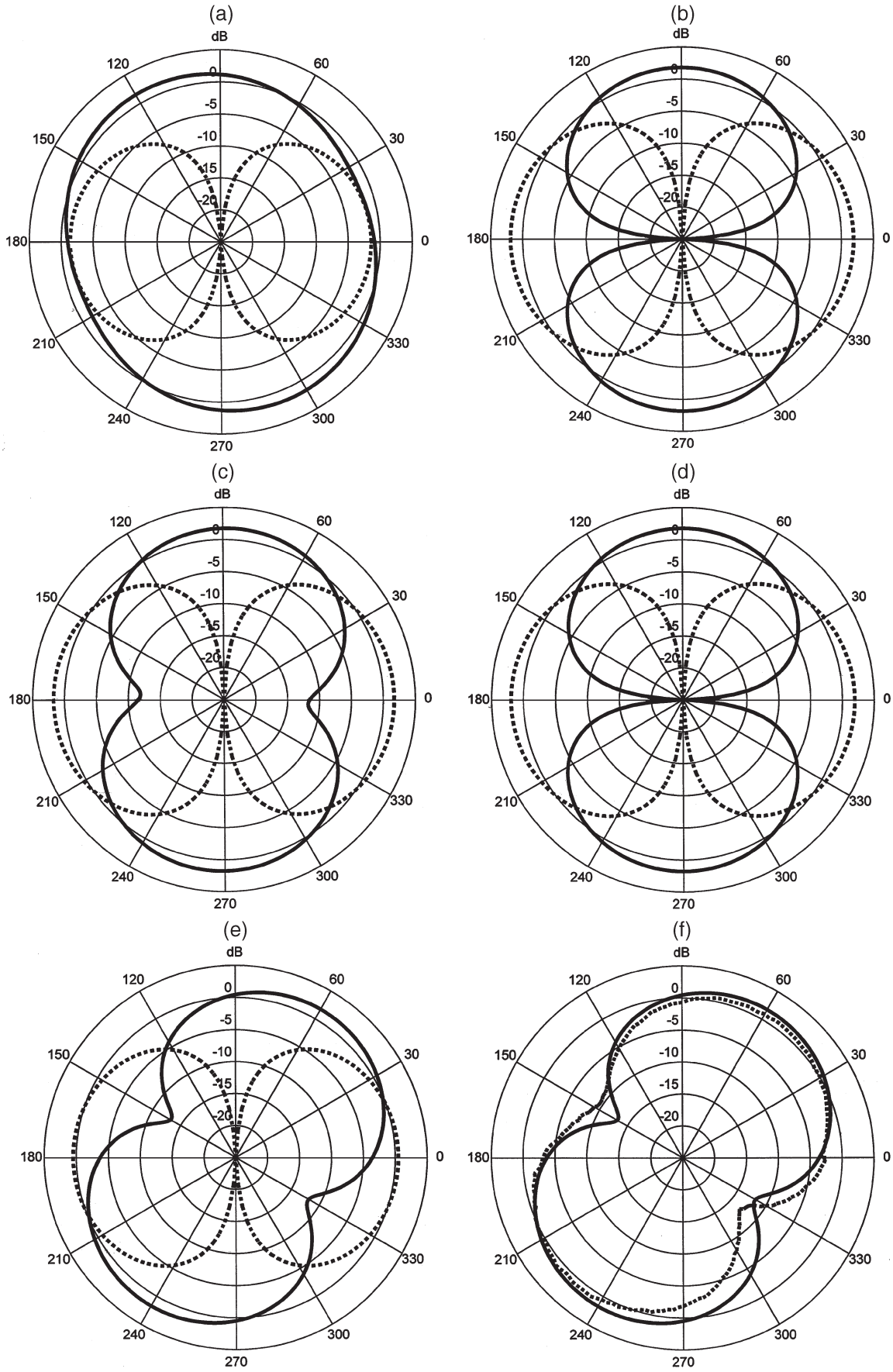

Fig. 6. (a)–(e) Computed radiation patterns. Solid line: $E_{\varphi}(\varphi, \theta = 90^{\circ})$. Dashed line: $E_{\theta}(\theta, \varphi = 90^{\circ})$. (f) Radiation patterns $E_{\varphi}(\varphi, \theta = 90^{\circ})$. Solid line: computed. Dashed line: measured.

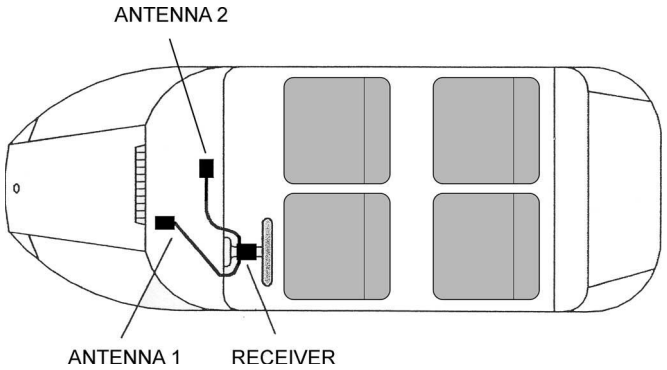

Fig. 7. Two examples of the antenna location in the car with a receiver module placed on the steering column and RF cable.

between the measured and the computed directionality [Fig. 6(f)] is quite good.

The best antenna for RKE automotive applications would obviously have an omnidirectional antenna radiation pattern. The antenna radiation patterns shown in Fig. 6 have significant dips in some angle directions. On the other hand, it is known that radiation patterns are very specific to the location of the antenna in (or on) the vehicle [11], [35]–[37] because reflections and shadowing effects can be significant. An antenna that is omnidirectional in free space has dips in the antenna pattern when placed in the vehicle. Therefore, the results shown in Fig. 6 can only be used as a guide for RKE mobile antenna design. Thus, our next step would be to mount a meander line antenna with an amplifier in the vehicle and measure performance for different antenna locations in the car.

It should be noted that according to our simulations, meander line antennas have very stable tolerances and do not require high quality inductors in the matching circuit. Therefore, meander line antennas are preferable in production processes, particularly in the vehicular applications that form our centers of interest.

VI. External Active Meander Line Antenna in the Car

The antennas described previously were designed for remote control vehicle applications. These applications use a "fob key" transmitting antenna (this fob key is often part of a house-and-office key chain that can be kept in a purse or pocket). These fob key antennas are generally loop antennas. They have omnidirectional antenna radiation patterns in the azimuth plane with the electric field vector orientation parallel to the azimuth (ground plane). In practical applications, the user could be holding the fob key in any orientation. Therefore, investigation of the receiving radiation antenna pattern in both azimuth and vertical planes is our prime interest.

We investigated an amplifier meander line [Fig. 1(e)] external antenna connected to the receiving control device through the 50-Ω cable. Two examples of the antenna location in the car with the receiver module placed on the steering column and RF cable route are shown in Fig. 7. It is common for DaimlerChrysler vehicles to have the RKE modules located on the steering column [38]. The RKE system described in [38] consists of an antenna and RF receiver with a digital processor integrated in one module. The separation of the antenna from the control module (Fig. 7) allows the placement of the antenna close to the car window. This reduces the shadowing effect of the car body and also allows installing the antenna, which is flat and printed, next to the interior body parts, so that it is completely hidden. Such design also reduces electromagnetic interference between the antenna and the electronic components of the RKE module and therefore extends the communication range between transmitter and receiver.

The amplifier for the antenna was designed using Genesys computer software from Eagleware Corporation [34]. Overall, amplifier properties were optimized to obtain noise impedance matching between the antenna and transistor stage, and power impedance matching between the amplifier and 50-Ω load. The amplifier consisted of a single-stage NE 662 transistor from California Eastern Laboratories coupled to a passive input matching circuit that provided a low-noise figure and to an output matching circuit that provided for maximum amplifier gain. The experimentally measured amplifier gain in the 315-MHz band was about 15 dB, whereas the noise figure of the amplifier was roughly 2 dB.

As previously emphasized, antenna pattern performances are very specific to the location of the antenna on a vehicle. Only experimentally determined electromagnetic field strengths around the vehicle with the antenna in the appropriate mounting position can reveal the antenna's true performance. In this case, the investigated unbalanced antenna, with a size of less than 1/10 of the free space wavelength, has a small ground plane. Unbalanced antennas are affected by the RF current flowing through the RF cable electrically connected to the receiver, such that a significant amount of radiation emanates from the RF cable. In this type of situations, direct connection of the coaxial cable to the antenna without the use of a balun can enhance antenna gain [39]. Thus, cable location is critical in the performance of the miniature antenna. Under such conditions, the only way to obtain a valid gain measurement is to test the antenna, which is connected to the receiver through the cable, while it is mounted in place on the vehicle. Therefore, all antenna performance measurements were made when the active receiving antenna was mounted in this fashion. A transmitting Yagi antenna with horizontal or vertical polarization was located at the far zone of the antenna-vehicle receiving system to provide signal power for the antenna pattern measurement.

A. Radiation Pattern Measurement Results

In accordance with supplier requirements, the antenna was to be placed under the front dash of the car. Radiation antenna pattern measurements were provided by a spectrum analyzer placed instead of the RKE module. The measured horizontal and vertical polarization field components in the xy plane for antennas 1 and 2 with a cable length of about 1.25 meters are presented in Fig. 8. Antennas and cable locations (cable location #1 for antenna 1 and cable location #4 for antenna 2) are shown in Fig. 7. Table III shows the average gain measurement results over 360° for several pseudorandom cable routes between the antenna and the receiver modules. Radiation patterns were clearly affected by changes in cable position and car body. The best location was that of antenna 1 with cable routing #2; the worst location was that of antenna 2 with cable routing #4. The difference between the average, over 360°, of the maximum and the minimum gain values was about 5 dB for vertical polarization and 2 dB for horizontal polarization. These results show that the proper choice of cable position in the car for small antennas can increase the antenna system gain by several decibels.

B. Signal-to-Noise Measurements

The noise performance of the active antenna prototype was measured in the car. The spectrum analyzer indicated that the average noise value was −102 dBm when the transmitting antenna was turned off.

The gain of the active antenna can be expressed as

$$G_{\mathrm{act}} = G_{\mathrm{pas}} \cdot G_{\mathrm{amp}} \tag{5}$$

where G_{pas} is the gain of the passive portion of the antenna and G_{amp} is the amplifier gain.

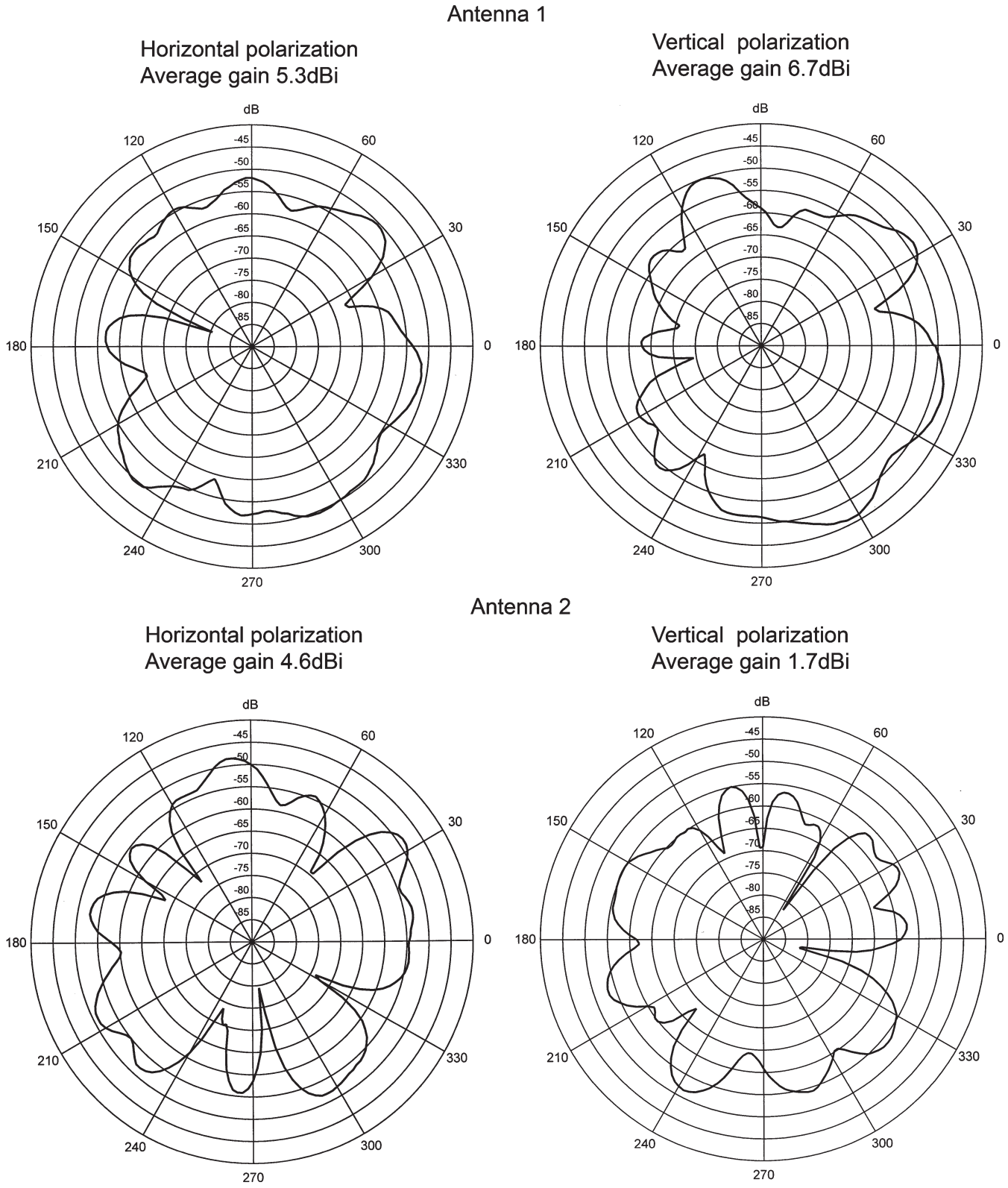

Fig. 8. Horizontal and vertical field components in the xy plane, measurement results.

It is known [40] that signal-to-noise ratio at the receiver output can be expressed as

$$q = \frac{\alpha \cdot \text{EIRP} \cdot G_{\text{act}}}{D^n \cdot (N_{\text{ant}} + k \cdot T \cdot B \cdot (F_{\text{rec}} - 1))} \tag{6}$$

where

EIRP	$= P_t \cdot G_t$; effective isotropic radiated power;
P_t	transmitting power;
G_t	gain of transmitting antenna;
α	$= (\lambda/(4 \cdot \pi))^2$; $\lambda =$ wavelength;
D	maximum range;

TABLE III
AVERAGE OVER 360° GAIN MEASUREMENT RESULTS FOR A FEW PSEUDORANDOM CABLE ROUTES BETWEEN ANTENNAS AND RECEIVER MODULE

	Antenna 1			Antenna 2		
Route #	#1	#2	#3	#4	#5	#6
Gain horizontal polarization (dBi)	5.3	6.6	4.8	4.6	6.5	8.7
Gain vertical polarization (dBi)	6.7	7.5	6.0	1.7	3.6	5.5

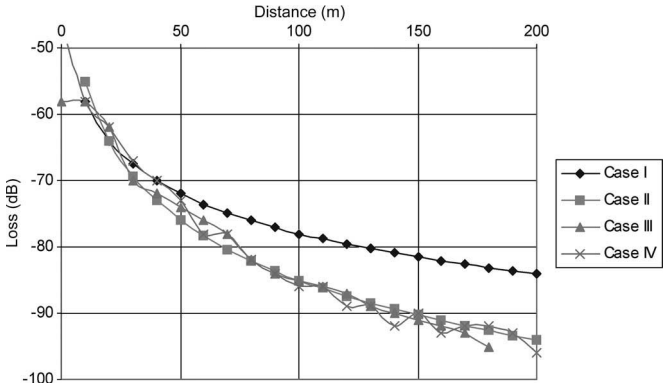

Fig. 9. Propagation loss dependence on distance.

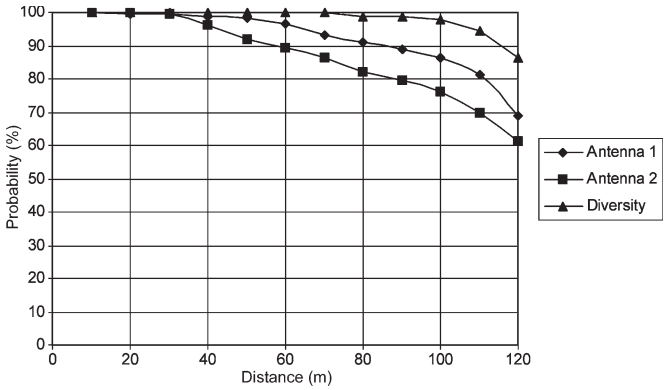

Fig. 10. Probability of detection (horizontal polarization) versus the distance between transmitter and RKE system.

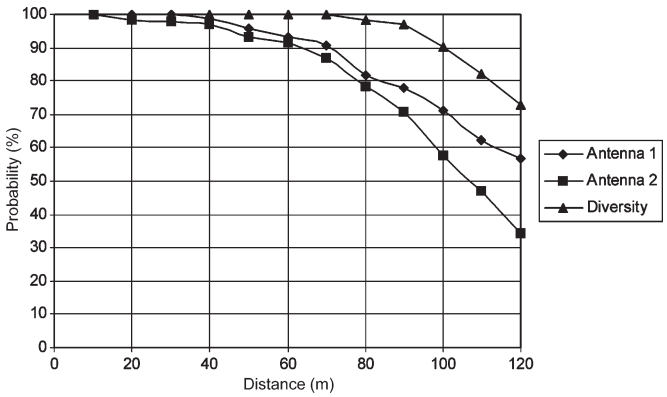

Fig. 11. Probability of detection (vertical polarization) versus the distance between transmitter and RKE system.

n constant that determines propagation losses in the real environment (free space, open area, urban area, etc.);
$N_{\rm ant}$ $= k \cdot T \cdot B \cdot F_{\rm amp} \cdot G_{\rm amp}$; residual noise level at the active antenna output;
k Boltzman's constant;
T ambient room temperature;
B equivalent bandwidth of the measuring device;
$F_{\rm rec}$ receiver noise figure;
$F_{\rm amp}$ amplifier noise figure.

As a rule, the noise figure $F_{\rm amp}$ of an active antenna with low-noise amplifier is satisfied by the following equation: $F_{\rm amp} \gg (F_{\rm rec} - 1)/G_{\rm amp}$. Using (6), the maximum range can be approximated as

$$D^n \approx \alpha \cdot \frac{\text{EIRP} \cdot G_{\rm act}}{q \cdot N_{\rm ant}}. \tag{7}$$

Fig. 9 reveals measurement results from our experiments that can be used to help estimate the n value in an open area. Four cases are considered.

Case 1 Free-space losses vary as C/D^2, where C is a constant that does not depend on the distance D between transmitter and receiver.
Case 2 Losses vary as C/D^3.
Case 3 Losses are measured when the fob key is located 1.5 m above the ground from the front side of the car in an open area while the RKE system is in the car.
Case 4 Losses are measured when the fob key is located 1.5 m above the ground from the rear side of the car in an open area while the RKE system is in the car.

It can be seen from the measurement results that value n can be chosen equal 3 for the open area.

According to supplier requirements and Federal Communications Commission (FCC) regulations, the EIRP must be less than -10 dBm for North America. Experiments show that in a real (not simulated) environment, with the fob key in a person's hand, the EIRP does not exceed -15 dBm. Thus, let us assume that EIRP $= -15$ dBm and $q = 5$ dB. For simplicity, we estimate the signal-to-noise ratio q at the receiver output to be 5 dB based on an assumption that the probability of bit error for pulse modulation signal is less than 0.01 [41]. For a frequency range of 315 MHz, $\alpha = -22$ dB. The experimental value of the residual noise level at the active antenna output $N_{\rm ant}$ is equal to -102 dBm. The active gain $G_{\rm act}$ of an antenna 1 with the cable location shown in Fig. 7 is a function of the observation angle, as presented in Fig. 8. Therefore, the maximum range according to (7) is also a function of the observation angle (as a rule, our angle position is a random value compared to the car when we want to, for example, open or close the door).

We can estimate the quality of the keyless entry system using the probability $P\ (D > L)$ that the range D is more than a certain value L. This probability is the ratio of the number M of the points in Fig. 8, for which the range D is more than L, to the total number M_o of the measuring points. Our turntable measures values with 2° steps over 360°. Therefore, M_o is equal to 180. As an example, graph 1 (horizontal polarization, antenna 1) and graph 2 (horizontal polarization, antenna 2), as presented in Fig. 10, show the probability $P\ (D > L)$ (in percentage scale) as a function of the range L (in meters). The same graphs for vertical polarization are shown in Fig. 11. Let us assume that

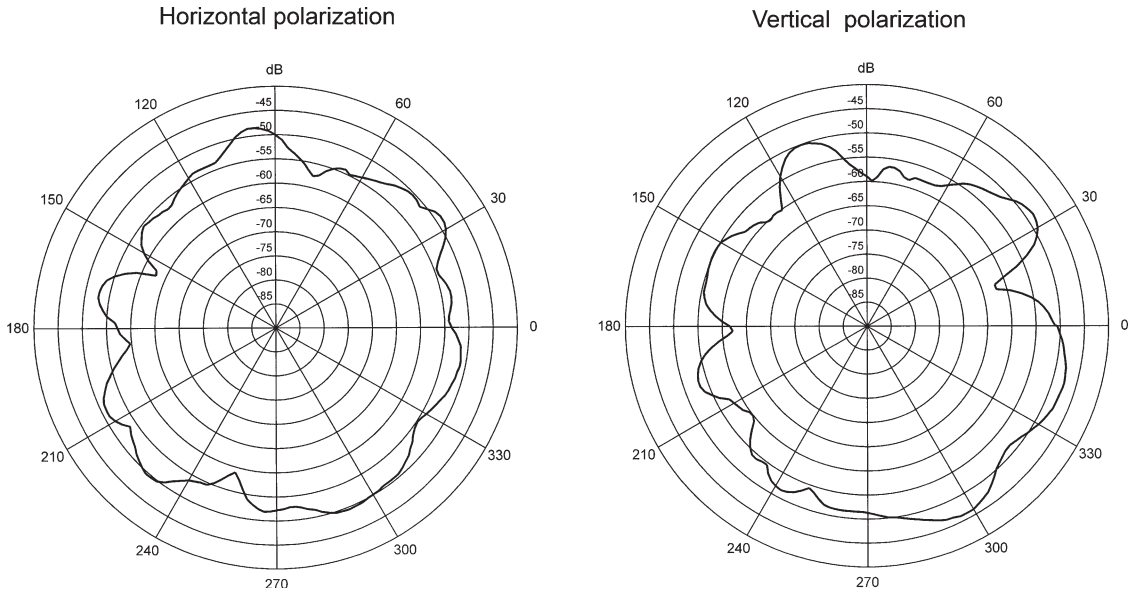

Fig. 12. Diversity antenna radiation pattern.

we want to estimate the probability that the maximum range would be more than 100 meters for antenna 1, as shown in Fig. 7. As observed in Figs. 10 and 11, the probability $P\ (D > 100\ \text{m})$ is 87% for horizontal polarization and 72% for vertical polarization. The antenna radiation patterns presented in Fig. 8 show that in some angle directions, the range decreases dramatically. For example, for an angle direction of 160° (Fig. 8, antenna 1, horizontal polarization), the antenna gain drops to the value of -45 dBi. Therefore, the range for this angle direction is about 3 m. It is possible to increase the range in these angle directions by using two antennas in a configuration known as a diversity antenna system.

C. Diversity Antenna Radiation Pattern

The diversity antenna concept presented here is given as follows: Periodically, the RKE module is connected to either the first or second antenna. The connection time with each antenna is long enough to receive the communication protocol. This logic excludes feedback information from the receiver, which is common in space diversity systems [41]. In this case, the diversity antenna radiation pattern is the overlap of the individual radiation patterns measured for antennas 1 and 2. Let us assume that we are using the two antennas shown in Fig. 7 for our diversity system. The curves presented in Fig. 12 show the overlap of the horizontal and vertical antenna radiation patterns presented in Fig. 8. As shown, the nulls in Fig. 8 are no longer presented in the diversity antenna radiation pattern shown in Fig. 12. By eliminating these nulls, the antenna directionality is more omnidirectional. This improvement translates to the increased communication range for the system. Graph 3 in Figs. 10 and 11 shows the probability P for this case. We can see that P for 100 m is increased to 98% for horizontal polarization and to 90% for vertical polarization.

VII. Conclusion

In this paper, miniature antennas for remote control automotive applications were investigated through both simulation and experimental analysis. Input impedance, radiation and loss resistance, efficiency, and gain of several geometries are presented. The VSWR as a function of the matching elements' tolerances was also examined. The research revealed that meander antennas have minimum VSWR fluctuations within allowable tolerances of the lumped matching elements. Therefore, small-size meander line antennas have very stable tolerances, do not require low-quality inductors in the matching circuits, and are preferable in production processes.

The performance of an active meander line antenna was measured in a car. The influence of the location of the antenna cable was also investigated. The cable position was found to have a strong effect on the antenna gain. The difference between the worst and best (from antenna gain point of view) cable locations was around 5 dB. By choosing an optimal antenna cable location, it is possible to increase the communication range.

The detection probability for a given radiation pattern was measured for different communication ranges. It was shown that using two antennas for RKE module operation (space diversity concept) significantly increases the communication range for angle directions where a system with one antenna gives reduced range.

References

[1] A. Bensky, *Short-Range Wireless Communications*. Eagle Rock, VA: LLH Technol., 2000.
[2] F. L. Dacus, "Design of short-range radio systems," *Microw. RF*, vol. 40, no. 9, pp. 73–80, Sep. 2001.
[3] W. Duerr and W. Menzel, "A low-noise active receiving antenna using a SiGe HBT," *IEEE Microw. Guided Wave Lett.*, vol. 7, no. 3, pp. 63–65, Mar. 1997.
[4] K. Smithin *Antennas for Low Power Applications*. Dallas, TX: RF Monolithic Inc., Fall 2000. [Online]. Available: www.rfm.com/corp/appdata/antenna.pdf
[5] K.-L. Wong, *Planar Antennas for Wireless Communications*. Hoboken, NJ: Wiley, 2003.
[6] B. Sun, Q. Liu, and H. Xie, "Compact monopole antenna for GSM/DCS operation of mobile handsets," *Electron. Lett.*, vol. 39, no. 2, pp. 1562–1563, Oct. 2003.
[7] Y. Kuo, T. Chiou, and K. Wong, "A novel dual-band printed inverted-F antenna," *Microw. Opt. Technol. Lett.*, vol. 31, no. 5, pp. 353–355, Dec. 2001.
[8] Y. Lin, H. Chen, and H. Chen, "A dual-band printed L-shaped monopole for WLAN applications," *Microw. Opt. Technol. Lett.*, vol. 37, no. 3, pp. 214–216, May 2003.
[9] H. Tung, C. Fang, and K. Wong, "An inverted-L monopole antenna loaded with a meandered wire for GSM/DCS dual-band mobile phones," *Microw. Opt. Technol. Lett.*, vol. 33, no. 3, pp. 212–214, May 2002.

[10] H. Chen, J. Chen, and Y. Cheng, "Modified inverted-L monopole antenna for 2.4/5 GHz dual-band operations," *Electron. Lett.*, vol. 39, no. 22, pp. 1567–1568, Oct. 2003.
[11] B. Al-Khateeb, V. Rabinovich, and B. Oakley, "An active receiving antenna for short range wireless automotive communication," *Microw. Opt. Technol. Lett.*, vol. 43, no. 4, pp. 293–297, Nov. 2004.
[12] J. Lee and S. Park, "The meander line antenna for bluetooth," *Microw. Opt. Technol. Lett.*, vol. 34, no. 2, pp. 149–151, Jul. 2002.
[13] C. Wang and C. Jou, "Compact microstrip meander antenna," *Microw. Opt. Technol. Lett.*, vol. 22, no. 6, pp. 413–414, Sep. 1999.
[14] H. Chen, "Triple-band triangular-shaped meander monopole antenna with two coupled lines," *Microw. Opt. Technol. Lett.*, vol. 37, no. 3, pp. 232–234, May 2003.
[15] M. Ali, M. Okoniewski, and S. Stuchly, "Study of a printed meander antenna using the FDTD method," *Microw. Opt. Technol. Lett.*, vol. 37, no. 6, pp. 440–444, Jun. 2003.
[16] G. Marrocoo, "Gain-optimized self-resonant meander line antennas for RFID applications," *IEEE Trans. Antennas Wireless Propag. Lett.*, vol. 2, no. 1, pp. 302–305, 2003.
[17] H. Nakano, H. Tagami, A. Yoshizawa, and J. Yamauchi, "Shortening ratios of modified dipole antennas," *IEEE Trans. Antennas Propag.*, vol. AP-32, no. 4, pp. 385–386, Apr. 1984.
[18] W. Choi, S. Kwon, and B. Lee, "Ceramic chip antenna using meander conductor lines," *Electron. Lett.*, vol. 37, no. 15, pp. 933–934, Jul. 2001.
[19] M. Ali, S. Stuchly, and K. Caputa, "An experimental study of small self-resonant antennas for wireless applications," *Microw. Opt. Technol. Lett.*, vol. 35, no. 2, pp. 143–145, Oct. 2002.
[20] S. Best, "A comparison of the performance properties of the Hilbert curves fractal and meander line monopole antennas," *Microwave Opt. Technol. Lett.*, vol. 35, no. 4, pp. 258–262, Nov. 2002.
[21] S. Best and J. Morrow, "Limitations of inductive circuit model representations of meander line antennas," in *Proc. IEEE Antennas Propag. Symp.*, Columbus, OH, Jun. 2003, pp. 439–442.
[22] T. Endo, Y. Sunahara, S. Satoh, and T. Katagi, "Resonant frequency and radiation efficiency of meander line antennas," *Electron. Commun. Jpn.*, vol. 83, pt. 2, no. 1, pp. 52–58, 2000.
[23] R. Azadegan and K. Sarabandi, "A Compact folded dipole antenna for wireless applications," in *Proc. IEEE Antennas Propag. Symp.*, Columbus, OH, Jun. 2003, pp. 439–442.
[24] M. Takiguchi and Y. Yamada, "Input impedance increase of a very small meander line antenna," in *Proc. IEEE Antennas Propag. Symp.*, Columbus, OH, Jun. 2003, pp. 856–859.
[25] T. Warnagiris and T. Minardo, "Performance of meandered line as an electrically small transmitting antenna," *IEEE Trans. Antennas Propag.*, vol. 46, no. 12, pp. 1797–1801, Dec. 1998.
[26] K. Ogawa, T. Uwano, and M. Takahashi, "A shoulder-mounted planar antenna for mobile radio applications," *IEEE Trans. Veh. Technol.*, vol. 49, no. 3, pp. 1041–1044, May 2000.
[27] H. A. Wheeler, "Small antennas," *IEEE Trans. Antennas Propag.*, vol. AP-23, no. 4, pp. 462–469, Jul. 1975.
[28] W. Geyi, "Physical limitations of antenna," *IEEE Trans. Antennas Propag.*, vol. 51, no. 8, pp. 1116–2123, Aug. 2003.
[29] A. Yaghjian and S. Best, "Impedance, bandwidth, and Q of antennas," in *Proc. IEEE Antennas Propag. Symp.*, Columbus, OH, Jun. 2003, pp. 501–504.
[30] R. C. Hansen, "Fundamental limitations in antennas," *Proc. IEEE*, vol. 69, no. 2, pp. 170–182, Feb. 1981.
[31] J. D. Kraus and R. J. Marhefka, *Antennas*. New York: McGraw-Hill, 2002.
[32] T. Tsukiji and S. Tou, "On polygonal loop antennas," *IEEE Trans. Antennas Propag.*, vol. AP-28, no. 4, pp. 571–575, Jul. 1980.
[33] Modelling of 3-D metallic structures with dielectric layers. *IE3D-Electromagnetic Simulation and Optimization Software*, Zeland Software Inc. [Online]. Available: www.zeland.com
[34] Genesys: High-speed linear circuit simulation, active and passive matching network synthesis, L-C filter synthesis. *Genesys: RF and Microwave Design Software*. Eagleware Corp. [Online]. Available: www.eagleware.com
[35] C. Hill and T. Kneisel, "Portable radio antenna performance in the 150, 450, 800 and 900 MHz Bands Outside and In-Vehicle," *IEEE Trans. Veh. Technol.*, vol. 40, no. 4, pp. 750–756, Nov. 1991.
[36] M. Daginnus, R. Kronberger, A. Stephan, J. Hopf, and H. Lindenmeier, "SDARS-antennas: Environmental influences, measurement, vehicle application investigations and field experiences," presented at the Society of Automotive Engineers World Congress, (SAE), Detroit, MI, Mar. 4–7, 2002, SAE Technical Papers Series, 2002-01-0120.
[37] K. Fujimoto and J. R. James, *Mobile Antenna Systems Handbook*. Boston, MA: Artech House, 1994, pp. 336–337.
[38] Burr *et al.*, "Column electronics control assembly," U.S. Patent 6 731 020 B2, May 4, 2004.
[39] H. Morishita, Y. Kim, and K. Fujimoto, "Design concept of antennas for small mobile terminals and the future perspective," *IEEE Antenna Propag. Mag.*, vol. 44, no. 5, pp. 30–43, Oct. 2002.
[40] J. Salter, *Specifying UHF Active Antennas And Calculating System Performance*, Jul. 2003, Research and Development British Broadcasting Corporation. White Paper 066.
[41] T. S. Rappoport, *Wireless Communications*. Englewood Cliffs, NJ: Prentice-Hall, 2002, pp. 340–343. 380-387.

Analysis of the Outage Probability for MIMO Systems With Receive Antenna Selection

Hao Shen and Ali Ghrayeb

***Abstract*—This paper presents a comprehensive analysis of the outage probability for multiple-input–multiple-output (MIMO) systems with receive antenna selection. In this analysis, it is assumed that 1) for a given M receive antennas, the receiver selects the best L antennas that maximize the capacity, 2) the channel state information is perfectly known at the receiver, but not at the transmitter, 3) the subchannels fade independently, and 4) the fading coefficients change very slowly such that averaging with respect to these coefficients is not possible. Under these assumptions, two upper bounds on the outage probability with receive antenna selection are derived. The first bound is used to show that the diversity order is maintained with antenna selection. The second bound is used to approximate the degradation in signal-to-noise ratio due to antenna selection. Furthermore, the asymptotic behavior of the outage probability for MIMO systems is analyzed as the number of transmit antennas tends to infinity. The asymptotic results presented are extended to the case with receive antenna selection. For all cases, explicit expressions for the threshold for the outage probability are derived. Several numerical examples that validate the analysis are also presented.**

***Index Terms*—Multiple-input–multiple-output (MIMO) channel, mutual information, outage probability, receive antenna selection, spatial diversity.**

I. Introduction

One of the main advantages of using multiple antennas at the transmitter and/or receiver is that it results in a drastic increase in the channel capacity, as shown by Telatar [1] and Foschini and Gans [2]. To this end, a number of papers have been published recently analyzing the capacity of multiple-antenna systems [3]–[7]. One of the drawbacks of employing multiple antennas, however, is the associated complexity. That is, the complexity that arises from employing a

Manuscript received October 7, 2004; revised March 29, 2005, August 18, 2005, December 6, 2005, and December 9, 2005. This work was supported in part by Natural Sciences and Engineering Research Council of Canada under Grant N00858. This work was presented in part at the IEEE Wireless Communications and Networking Conference (WCNC), New Orleans, LA, March 2005. The review of this paper was coordinated by Prof. M. Juntti.

H. Shen was with the Department of Electrical and Computer Engineering, Concordia University, Montreal, QC H3G 1M8, Canada. He is now with General Electric (GE), Montreal, QC, Canada (e-mail: howard.shen@ge.com).

A. Ghrayeb is with the Department of Electrical and Computer Engineering, Concordia University, Montreal, QC H3G 1M8, Canada (e-mail: aghrayeb@ece.concordia.ca).

Digital Object Identifier 10.1109/TVT.2006.877703